J. PHYS IV FRANCE 7 (1997)
Colloque C3, Supplément au Journal de Physique III d'août 1997

Adiabatic Shear in Remco Iron and Quenched and Tempered 4340 Steel

C.R. Mason, M.J. W[illegible]wick and P.J. Gallagher*

Department of Mechanical and Aerospace Engineering, Carleton University, 1125 Colonel By Drive, Ottawa, Canada K1S 5B6
** Defense Research Establishment Suffield, Box 4000, Medicine Hat, Alberta, Canada T1A 8K6*

Abstract. Adiabatic shear localization is studied in two ferrous metals, Remco Iron, a high purity alpha iron, and 4340 steel, quenched and tempered at 650°C. Punching-shear experiments are performed in a compressive split-Hopkinson bar producing shear strain rates of 45,000 s^{-1}. Optical and scanning electron microscopy was performed on the deformed shear specimens to determine the extent of shear localization and mode of failure. Experimental evidence showed that the 4340 steels were susceptible to localization through adiabatic shear banding, however, the Remco iron did not exhibit fine shear bands typical of localization.

Finite element simulations of the experiments were performed utilizing a user material subroutine developed as part of this research. This constitutive routine incorporates two adiabatic shear failure criteria: (i) maximum shear stress and (ii) flow localization theory. These criteria proved to be capable of predicting the onset of an instability, however, the deformation which follows the instability was only moderately predicted well.

Résumé. Le phénomène de la localisation du cisaillement adiabatique est étudié pour deux métaux ferreux. Le fer Remco, un fer de haute pureté de type alpha et l'acier 4340, trempé et revenu à 650 C. Des essais de cisaillement par poinconnage ont été effectués avec un système de barres Hopkinson de type compression produisant des taux de déformation par cisaillement de l'ordre de 45,000 s^{-1}. La microscopie optique et à balayage électronique ont été utilisées sur des échantillons déformés par cisaillement pour déterminer l'étendue de la localisation du cisaillement et le mode de rupture. Les données expérimentales démontrent que les aciers de type 4340 sont susceptible à la localisation par bandes de cisaillement adiabatique, et que par contre, le fer Remco n'a pas affiché des bandes de cisaillement typiques au phénomène de localisation.

Des simulations par éléments finis des mêmes expériences ont été effectuées en utilisant une sous-routine maison pour le matériau développée dans le cadre de cette recherche. Cette sous-routine constitutive incorpore deux critères de rupture par cisaillement adiabatique: (I) la contrainte maximale en cisaillement et (II) la théorie de la déformation plastique par localisation. Ces critères ont démontrés leur capacité à prédire adéquatement le début de l'instabilité, mais par contre, la déformation subséquente à l'instabilité n'a été prédite que de façon relativement bonne.

1. INTRODUCTION

In metals remaining ductile under high strain rate conditions, failure occurs through either ductile fracture or adiabatic shear localization. The former mechanism occurs through the nucleation, growth, and coalescence of microvoids to form a crack. Adiabatic shear localization [1, 2, 3] is a thermal instability process in which a rapid temperature rise due to plastic work couples with thermal softening to cause uniform deformation to collapse into narrow bands of intense shear within which material ductility is exhausted.

This paper presents results from a recent study [4] of adiabatic shear in a series of ferrous alloys, annealed Armco and Remco irons, shock-hardened Remco iron, and 4340 steel heat treated to a range of hardnesses. In particular, results are given for annealed Remco iron and 4340 steel quenched and tempered at 650°C. These materials were tested under punching-shear deformation (Figure 1) utilizing a compressive split Hopkinson bar (CSHB) to generate shear strain rates of roughly 45,000 s^{-1}. The specimen is sheared between a punch and ring die assembly similar to that used by Meyer and Manwaring [5].

Metallographic examination of deformed specimens was performed to determine the extent and

102-02586/

structure of the adiabatic shear bands. Supporting numerical simulations of the experiments were also undertaken utilizing a user material model developed as part of this research. Predictions of adiabatic shear failure were performed using (i) attainment of maximum shear stress (MSS) or onset of strain softening and (ii) a flow localization criterion proposed by Semiatin et al [6]. It is well established that the instability associated with the onset of strain softening generally precedes adiabatic shear localization. Of interest in this research is the extent of deformation after instability and whether simplified criteria such as MSS can be used in finite element codes to predict shear failure in engineering calculations.

2. MATERIALS

The Remco iron was received in the hot-rolled condition with a plate thickness of 25 mm. The plate was annealed at 550°C for 2 hours in a nitrogen atmosphere to relieve residual stresses due to hot rolling. The plate exhibited a varying grain size through-thickness.

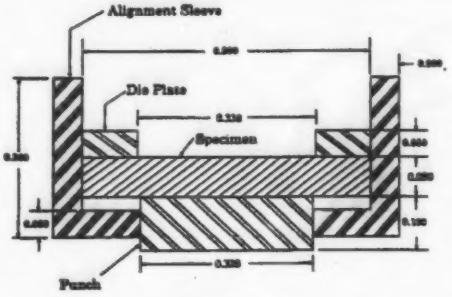

The central portion of the plate had a fine grain structure (30-35 μm) while there was a coarse grain structure (350-500 μm) near the surfaces of the plate extending to a depth of 3 to 5 mm below the surface. The specimens discussed in this paper were all taken from the fine grained region of the plate. The 4340 specimens were austenitized at 870°C for 1 hour and then oil quenched. After quenching, the specimens were tempered for 2 hours at 650°C to produce a tempered martensite microstructure with a measured hardness of 28 Rc.

Figure 1: Shear specimen assembly

3. EXPERIMENTS

Disk-shaped specimens were machined from the Remco iron and 4340 steel with dimensions shown in Figure 1. The punch-specimen-die assembly was tested in compression using the CSHB at Carleton University. The plexiglass alignment sleeve is used to concentrically align the assembly within the Hopkinson bars.

From the dimensions in Figure 1, the radial clearance, δ, between the punch and die is 0.13 mm (0.005"). This clearance is the effective gauge length for the shearing process; thus, the nominal shear strain rate becomes

$$\gamma = \frac{\Delta v}{2\delta} \tag{1}$$

where Δv is the rate of closure between the Hopkinson bar ends.

4. MODEL

Finite element simulations of the shear specimens were performed using the LS-DYNA2D [7] explicit dynamic finite element code. Figure 2 shows the finite element mesh used to model the die-specimen-punch assembly adopted in this research. Figure 3 shows the shear zone and the punch and die radii in more detail. The mesh within the shear zone is extremely fine with an element size of 25 μm.

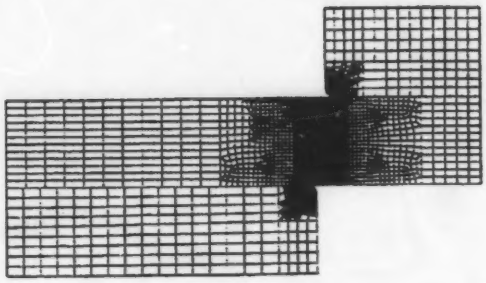

Figure 2: Finite element mesh used to model the die-specimen-punch assembly

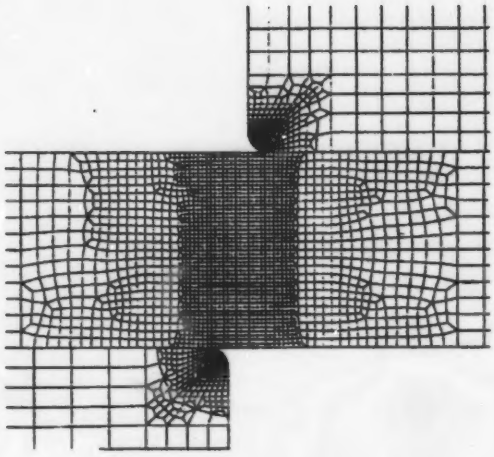

Figure 3: Close up view of shear region in the die-specimen-punch assembly

Velocity boundary conditions, consistent with the measured bar-end velocities, were prescribed on the punch and die faces in contact with the Hopkinson bars. Penalty function-based intermittent contact boundary conditions, known as slide lines, were defined along the die-specimen and the specimen-punch interfaces. An automatic contact option was utilized which updates contact definitions to account for element failure since the adiabatic shear band will cut the contact boundary once failure initiates.

4.1 Constitutive Model

The specimens were modelled using a user material subroutine or umat written as part of this research. The materials were treated as isotropic and obeying a Mises yield criterion. The constitutive response of the Remco iron was modelled using the Goldthorpe-modified form [8] of the Zerilli-Armstrong [9] equation. The 4340 steel was modelled using the Johnson-Cook model and constants given in [10] for the quenched and 650°C tempered condition.

Calculations utilizing the MSS criterion for failure assumed that failure through adiabatic shear would ensue once the rate of thermal softening overcomes the rate of strain hardening,

$$\frac{d\sigma}{d\varepsilon}\Big|_{d\dot{\varepsilon}=0} = \frac{\partial\sigma}{\partial\varepsilon} + \sigma\,\frac{\partial\sigma}{\partial T}\,\frac{1}{\rho C_p} < 0 \qquad (2)$$

in which σ and ε are the effective stress and strain, T is the temperature, ρ the density, and C_p is the specific heat. The first term on the right hand side is the rate of work hardening and the second term is the rate of thermal softening. When $\partial\sigma/\partial\varepsilon|_{d\dot{\varepsilon}=0} > 0$ the deformation is said to be stable; however, if $\partial\sigma/\partial\varepsilon|_{d\dot{\varepsilon}=0} < 0$ adiabatic shear is able to occur. In the event of an instability, the stresses in the element are relaxed to zero and the element is deleted from the calculation. A further condition on this instability criterion was also considered which required that the shear strain rates be high in order for the element to be considered a candidate for adiabatic shear failure. Simply put, an element must satisfy

$$\gamma_p > \gamma_{crit} \tag{3}$$

in addition to equation (2) prior to deletion. Here, γ_p is the principal shear strain rate (generally smoothed over a number of time steps) and γ_{crit} is a minimum critical shear strain rate, specified as a fraction of the nominal rate from the experiments.

Recognising that the onset of a thermal instability is not a sufficient condition for localization, a second criterion, as proposed by Semiatin et al [6], was considered. In their model of localization, deformation is assumed to occur in a defect-containing inhomogeneous band within a uniformly deforming region. They introduce a parameter α describing the ratio of strain rates and strains between the inhomogeneous and homogeneous regions, calculated here [11] as

$$\alpha = \frac{\delta \ln \dot{\varepsilon}}{\delta \varepsilon} = \left(- \frac{\partial \sigma / \partial \varepsilon}{\partial \sigma / \partial \dot{\varepsilon}} - \frac{\partial \sigma / \partial T}{\partial \sigma / \partial \dot{\varepsilon}} \frac{dT}{d\varepsilon} \right) \frac{1}{\dot{\varepsilon}} \tag{4}$$

where δ refers to the difference between quantifies inside and outside of the inhomogeneity. Through comparison with experiments on heat treated 4340 steels, Semiatin et al [6] suggest that conditions for which α ranged between 3-4 would lead to adiabatic shear localization.

5. RESULTS

Figures 4 and 5 are optical micrographs showing the shear regions from Remco iron and 4340 steel specimens. The 4340 steel shows evidence of martensitic transformation bands indicative of a sharp temperature rise associated with deformation collapsing into narrow shear bands. In contrast, the Remco iron exhibits relatively diffuse shear deformation and does not appear to localize. Final separation across the shear region occurs through ductile fracture as evidenced by the dimpled fracture surfaces (not shown) for both materials.

Figure 6 plots the nominal shear stress-strain response from the experiments and MSS predictions using equations (2) and (3) for annealed Remco iron. The experiments exhibit mechanical instability (softening behaviour) at a shear strain of roughly 0.8 and final fracture at roughly 3.0. The predictions employing $\gamma_{crit} = 0$ show very low ductility since extensive erosion of the mesh occurs in regions away from the shear band (Figure 7(a)). Calculations employing $\gamma_{crit} = 28, 125\ s^{-1}$, or 62.5% of the nominal strain rate, capture the onset of the instability and the subsequent ductility relatively well. The use of γ_{crit} also reduces the erosion of elements not undergoing shear as seen by comparing Figures 7(a) and (b).

Figure 8 presents the measured and predicted nominal shear stress-strain behaviour for the 4340 steel. The ductility is considerably less than for the Remco iron due to the higher initial hardness and lower work hardening response. The MSS criterion predicts an earlier onset of instability and overpredicts the strain to initiate failure compared to the experiment. Simulations using the α localization parameter gave similar ductility predictions for the 4340 steel compared to the MSS predictions. Values of α in the range of 3-4 were reached which are sufficient to cause localization as suggested by Semiatin et al [6] and in accord with the narrow shear localization bands in Figure 5. For the case of Remco iron, predicted values of α only slightly exceeded zero suggesting that conditions for shear localization were not met. This prediction is also in agreement with the observed diffuse shear seen in Figure 4.

6. DISCUSSION AND CONCLUSIONS

The present research has served to highlight differences in localization behaviour between the strongly hardening Remco iron and the weakly hardening heat treated 4340 steel. The localization parameter α is in general accord with the experimental observations, distinguishing between localized and non-localized deformation.

The use of the MSS instability criterion provided reasonable predictions of ductility when used in conjunction with a minimum shear strain rate requirement (γ_{crit}). This criterion is computationally

Figure 4: Optical micrograph showing shear region in annealed Remco iron

Figure 5: Optical micrograph showing sheared region in quenched and 650°C tempered 4340 steel

inexpensive and is attractive for engineering calculations of impulsive events involving adiabatic shear failure. The reader is cautioned, however, that this criterion can result in unrealistically low predictions of ductility in materials exhibiting low or negative work hardening after first yield such as shock-hardened Remco iron [4].

Acknowledgements

Financial support for this research was provided by the Natural Sciences and Engineering Council of Canada, the Defense Research Establishment Suffield, and the Australian Defence Science and Technology Office (Dr. Norbert Burman). The Remco iron used in this work was provided by Dr. George Weston of DSTO. The authors thank Ms. Christie Egbert for her assistance in the preparation of this manuscript.

References

[1] Timothy, S.P., *Acta Metall.*, **35** (1987) 301-306.
[2] Staker, M.A., *Acta Metall.*, **29** (1981) 683-689.
[3] Rogers, H.C., in Material Behaviour under High Stress and Ultrahigh Loading Rates, ed. J. Mascull, and U. Weiss, 1983, Pg. 101-118.
[4] Mason, C.R., Prediction of Adiabatic Shear in 4340 Steel, Remco and Armco Irons, M.Eng. Thesis, Carleton University, 1997.
[5] Meyer, L.W. and Manwaring, S., in Metallurgical Applications of Shock Wave and High-Strain-Rate Phenomena, eds. L.E. Murr, K.P. Staudhammer, and M.A. Meyers, (Marcel Dekker Inc. 1986) pp. 657-674.
[6] Semiatin, S.L., Staker, M.R., and Jonas, J.J., *Acta Metall.*, **32** (1984) 1347-1354.
[7] Hallquist, J.O., Users Manual, Livermore Software Technology Corporation, 1993.

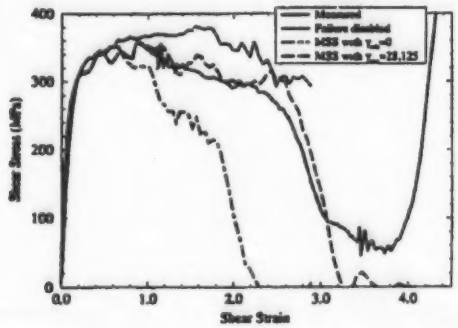

Figure 6: Nominal shear stress-strain curve for numerical model using the MSS criterion and experiment for annealed Remco iron

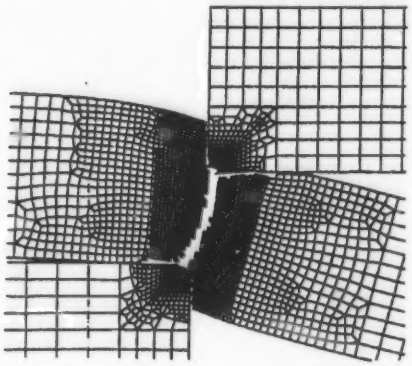

Figure 7a: Predicted crack using MSS criterion with $\dot{\gamma}_{crit}$ = 0 for Remco iron

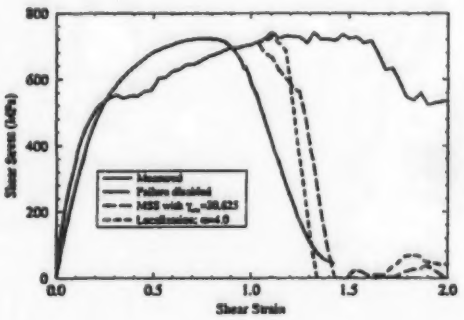

Figure 8: Nominal shear stress-strain curve for numerical using MSS and localization criteria and experiment for quenched and 650°C tempered 4340 steel.

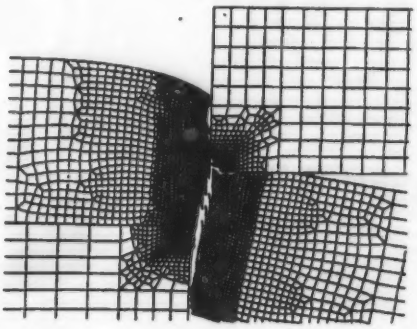

Figure 7b: Predicted crack using MSS criterion with $\dot{\gamma}_{crit}$ = 28.125 s^{-1} for Remco iron

[8] Goldthorpe, B.D., in 3rd International Conference on Mechanical and Physical Behaviour of Materials Under Dynamic Loading - DYMAT 91, (Les Editions de Physique, 1991) pp. 829- 835.

[9] Zerilli, F.J., and Armstrong, R.W., *J. Appl. Phys.*, **61** 5 1987, Pg. 1816-1825.

[10] Johnson, G.R. and Cook, W.H., in ADPA 7th International Symposium of Ballistics Proceedings, (1987), pp. 1816-1825.

[11] Ning, Q., Numerical and Experimental Simulation of Adiabatic Shear Localization in Tantalum and Armco Iron, Ph.D. Thesis, University of Waterloo, 1993.

#507082